

Improved Nearside-Farside Method for Elastic Scattering Amplitudes

R. Anni*

Dipartimento di Fisica dell'Università and Istituto Nazionale di Fisica Nucleare, I73100 Lecce, Italy

J. N. L. Connor[†] and C. Noli

Department of Chemistry, University of Manchester, Manchester M13 9PL, United Kingdom

(Dated: July 18, 2002)

A simple technique is described that provides an improved nearside-farside (NF) method for elastic scattering amplitudes. The technique, involving the novel resummation of a Legendre partial wave series, reduces the importance of unphysical contributions to NF subamplitudes, which can arise in more conventional NF decompositions. Detailed applications are made to a strong absorption model and to a $^{16}\text{O} + ^{16}\text{O}$ optical potential at $E_{\text{lab}} = 145$ MeV. We also discuss $^{16}\text{O} + ^{16}\text{O}$ at $E_{\text{lab}} = 480, 704, 1120$ MeV, and $\alpha + ^{12}\text{C}$, $\alpha + ^{40}\text{Ca}$, both at $E_{\text{lab}} = 1370$ MeV.

PACS numbers: 24.10.Ht, 25.70.Bc, 34.50.-s, 03.65.Sq

I. INTRODUCTION

In heavy-ion, atomic and molecular collisions, an elastic differential cross section, $\sigma(\theta)$, where θ is the scattering angle, is often characterized by a complicated interference pattern. This complicated structure makes it difficult to understand the physical phenomena involved in the scattering process, as well as the links between $\sigma(\theta)$ and the properties of the model that describes the phenomenon.

In some cases, semiclassical methods [1] explain the scattering pattern as the interference between simpler, and slowly varying, subamplitudes. If we ignore the complication that, in some angular regions, uniform asymptotic techniques are necessary, then the semiclassical subamplitudes arise mathematically from saddle points or poles, which account physically for contributions from reflected, refracted or generalized diffracted semiclassical trajectories [2]. The subamplitudes can be conveniently grouped into two types: those arising from semiclassical trajectories which initially move in the same half plane as the detector (N or nearside trajectories) and those from the opposite half plane (F or farside trajectories).

Semiclassical methods are not always simple to apply and sometimes they have a limited range of applicability. Their limitations are determined by the range of validity of the (presently known) asymptotic techniques that are used to approximate the original quantum mechanical problem.

In order to overcome these difficulties, it is common practice to apply to the elastic scattering amplitude, $f(\theta)$, a NF method that was proposed by Fuller[3] more than 25 years ago. The Fuller NF method has the merit of being simple and, although inspired by the semiclassical theories, it uses only scattering matrix elements S_l calculated (or directly parametrized) by exact quantum

mechanics. The NF subamplitudes are obtained by exact summation of NF partial wave series (PWS), thereby bypassing problems associated with the applicability and validity of semiclassical techniques, e.g. using approximate S_l , replacing the PWS by integrals, using stationary phase integration, etc.

The Fuller method is based on a splitting of the Legendre polynomials, $P_l(\cos \theta)$, in the PWS of $f(\theta)$, into traveling angular wave components, with the traveling angular waves consistent with detailed semiclassical analyses of scattering from impenetrable and transparent spheres [2].

The Fuller method was [4, 5] and continues to be widely used; indeed the ISI Web of Science reports about 140 citations since 1981 to Fuller's seminal work (for more recent examples see [6, 7, 8, 9, 10, 11] and references therein). The success of the method depends, apart from its simplicity, on its remarkable capability of physically explaining complicated interference patterns in cross sections as arising from the interference between NF subamplitudes having simple properties. In particular, the NF cross sections are often less structured and more slowly varying with θ than is the full cross section. Even though no semiclassical technique has been used, these NF subamplitudes can often be given a physical interpretation (in analogy with results from semiclassical methods) as contributions from simple scattering mechanisms, which then allows a good understanding of the angular scattering.

In the light of these unquestionable successes, it is desirable to extend the validity of the Fuller approach to cases where the original Fuller method is not (physically) satisfactory, for example, it may produce oscillatory and rapidly varying NF cross sections, when the full cross section is monotonic and slowly varying with θ . Examples of these shortcomings have been known for a long time. One classic example is pure Coulomb scattering. For repulsive Coulomb potentials only a N contribution is expected semiclassically ([1], p. 56), whereas the Fuller NF method yields also a F contribution [3]. As a result, the NF cross sections are less simple than the full

*Electronic address: Raimondo.Anni@le.infn.it

[†]Electronic address: J.N.L.Connor@Manchester.ac.uk

one. In this case, the unsatisfactory effects are, however, confined to a restricted backward angular region ([3], p. 1564). Another more striking example is observed in the scattering by a uniformly charged sphere ([4], p. 154, Fig. 26). In this case, the ratio of the full cross section to the Rutherford one decreases monotonically into the shadow of the Coulomb rainbow. In contrast, the N ratio closely follows the full ratio up to $\theta \approx 40^\circ$ when it becomes approximately constant (i.e. independent of θ), being approximately equal to the F ratio.

A similar effect is also observed in the angular distributions for a strong absorption model (SAM) with a two parameter (Λ and Δ) symmetric S matrix element and Fermi-like form factors [12]. For a fixed value of the cut-off parameter Λ and for a sufficiently large value of the diffuseness parameter Δ , the Fuller NF cross sections show an almost exponential decline up to a certain θ (which decreases with increasing Δ). At larger angles, the NF cross sections are greater than the full cross section, which continues its oscillatory exponential decline.

Similar striking effects appear at high energies and for large scattering angles in the NF cross sections of α particles and light heavy-ions scattered by nuclei using optical potentials. Less striking, but still disturbing, effects are also observed, at lower energies, in some N cross sections for the optical potentials used to fit recent data of light heavy-ion scattering [6, 7, 9, 11]. Typical N cross sections rapidly decrease from 0° and from 180° . The two branches meet in the crossing region where an interference pattern appears, with strong oscillations over an extended range of angles.

In this paper, we show how some of these shortcomings can be removed using a new NF method [13], based on an *improved modified resummation* of the PWS. The new method is a development of the Hatchell [12] idea of incorporating the Yennie, Ravenhall and Wilson (YRW) [14] resummation technique into the NF formalism. The limitations of the NF Hatchell resummation technique have been discussed [15, 16, 17] and a *modified* NF YRW resummation procedure, depending on two parameters α and β , was proposed [18, 19] to bypass the difficulties with the original NF YRW approach. The possibility of further *improving* the modified YRW resummation procedure, using different resummation parameters $\alpha_1, \alpha_2, \dots$ and β_1, β_2, \dots , together with a rule to fix the value of these parameters [13], is discussed in the present work.

For all three NF methods, Fuller, Hatchell and ours, the starting point is the quantum mechanical PWS for the full scattering amplitude $f(\theta)$,

$$f(\theta) = \frac{1}{2ik} \sum_{l=0}^{\infty} a_l P_l(\cos \theta), \quad (1)$$

where k is the wavenumber, $P_l(\cos \theta)$ is the Legendre polynomial of degree l and a_l is given in terms of the scattering matrix element S_l by:

$$a_l = (2l+1)(S_l - 1). \quad (2)$$

In the following, we will write $x = \cos \theta$. For future convenience, we recall that the PWS (1), considered as a distribution, converges to its exact value for $\theta \neq 0$, upon dropping the 1 in the term $S_l - 1$ on the r.h.s of (2). The omitted amplitude is proportional to the Dirac delta function $\delta(1-x)$ (e.g. see [1], p. 52). We also recall that the PWS (1), considered as a distribution, is convergent if S_l is asymptotically Coulombic [20].

In Sec. II, we briefly outline the original Fuller NF method, and show that unsatisfactory results are obtained for seven collision systems, which are different from those considered in [13]. In Sec. III, we discuss a modification of the Fuller NF technique proposed in Refs. [16, 17, 18, 19] and present an improved modified method. Our new method is very effective in cleaning unphysical contributions from NF cross sections for the seven examples where the usual Fuller technique gives unsatisfactory results. Our conclusions are in Sec. IV.

II. LIMITATIONS OF THE FULLER NF METHOD

A. Introduction

The Fuller NF decomposition is realized by splitting in (1) $P_l(x)$, considered as a standing angular wave, into traveling angular wave components

$$P_l(x) = Q_l^{(-)}(x) + Q_l^{(+)}(x), \quad (3)$$

where (for $x \neq \pm 1$)

$$Q_l^{(\mp)}(x) = \frac{1}{2} [P_l(x) \pm \frac{2i}{\pi} Q_l(x)], \quad (4)$$

with $Q_l(x)$ the Legendre function of the second kind of degree l .

Inserting (3) into (1) splits $f(\theta)$ into the sum of two subamplitudes

$$f(\theta) = f^{(-)}(\theta) + f^{(+)}(\theta), \quad (5)$$

with

$$f^{(\mp)}(\theta) = \frac{1}{2ik} \sum_{l=0}^{\infty} a_l Q_l^{(\mp)}(x). \quad (6)$$

Note that, by construction, the decomposition (5) is *exact*. Also we will obtain an exact decomposition, by using in place of the $Q_l^{(\mp)}(x)$ in (3), any pair of functions whose sum is $P_l(x)$. The property of the $Q_l^{(\mp)}(x)$ that makes the splitting (3) important, is the asymptotic result

$$Q_l^{(\mp)}(x) \sim \sqrt{\frac{1}{2\pi\lambda \sin \theta}} \exp[\mp i(\lambda\theta - \frac{\pi}{4})], \quad (7)$$

for $l \sin \theta \gg 1$, where $\lambda = l + \frac{1}{2}$. In particular, (7) allows $(-)$ to be identified with N scattering and $(+)$ with F

scattering ([4], p. 121). In the semiclassical theory, the splitting of $P_{\lambda-\frac{1}{2}}(x)$ into the sum of $Q_{\lambda-\frac{1}{2}}^{(\mp)}(x)$, or the related splitting obtained from the asymptotic expansions of these functions [1], plays a crucial role in deriving the semiclassical subamplitudes. In particular, the NF semiclassical subamplitudes arise from terms originally containing $Q_{\lambda-\frac{1}{2}}^{(\mp)}(x)$, or their asymptotic expansions (7). These facts raise the hope that the direct calculation of the $f^{(\mp)}(\theta)$ from their PWS representation in (6) will separate the NF contributions to $f(\theta)$, thereby avoiding problems connected with the applicability or validity of the semiclassical theory.

In order to make this hope mathematically rigorous, one should prove that it is possible to perform on the PWS, written in terms of the $Q_l^{(\mp)}(x)$, the same manipulations that are used in deriving the complete semiclassical decomposition of $f(\theta)$. These manipulations are essentially path deformations in λ of the integrals into which (1) can be transformed, using either the Poisson sum formula ([2], p. 45) or the Watson transformation ([2], p. 49). The consequences of these path deformations depend on the properties of the terms in the PWS when they are continued to real or complex values of λ from the initial physical half integer λ values. The splitting of $P_l(x)$ into the $Q_l^{(\mp)}(x)$ modifies these properties and can cause the appearance of unphysical contributions in the $f^{(\mp)}(\theta)$, which cancel out in $f(\theta)$ (these contributions are not expected to be present in the semiclassical subamplitudes).

In spite of these possible limitations, extensive experience with the Fuller NF method has demonstrated that the method is usually reliable, in the sense that it often decomposes $f(\theta)$ into simpler NF subamplitudes, apparently free from unphysical contributions arising from the above mathematical difficulties. However for a few examples, some of which were mentioned in Sec. I, the Fuller NF subamplitudes can be directly compared with the corresponding exact analytical, or semiclassical, results and disagreements are observed.

Fortunately, the Fuller NF subamplitudes contain information that allows one to recognize the unphysical nature of the undesired contributions. Suppose $f^{(+)}(\theta)$, or $f^{(-)}(\theta)$, contains a single semiclassical contribution from a stationary phase point at $\lambda(\theta)$. Then the derivative with respect to θ of the phase of $f^{(+)}(\theta)$, or $f^{(-)}(\theta)$, is equal to $\lambda(\theta)$, or $-\lambda(\theta)$, respectively ([1], p. 57). Following Fuller we will call this derivative the *Local Angular Momentum* (LAM) for the F (or N) subamplitude; it depends on θ . Usually, only for a generalized diffracted trajectory, arising from a simple pole, is the LAM expected to be constant, being equal to the angular momentum of the incoming particle responsible for the diffraction.

In the semiclassical regime, this constant value is expected to be large. Because of this, if we observe that, in a certain θ range, $\text{LAM} \approx 0$, this can be considered a warning for the unphysical nature of the N or F subamplitudes in that range of θ . This occurs for the LAM of

the Fuller Coulomb F subamplitude, and for the NF subamplitudes of the SAM in the angular region where the NF cross sections contain unphysical contributions [13]. In both cases, this decoupling of θ from LAM, together with the fact that the full cross section is simpler than the NF ones, suggests the unphysical nature of the NF subamplitudes.

We show below for seven collision systems, different from those considered in [13], how unphysical NF contributions manifest themselves. The seven collision systems are; (a) a simple SAM model, (b) $^{16}\text{O} + ^{16}\text{O}$ at $E_{\text{lab}} = 145$ MeV, using the WS2 optical potential of Ref. [7], and (c) more briefly, $^{16}\text{O} + ^{16}\text{O}$ at $E_{\text{lab}} = 480, 704, 1120$ MeV, and $\alpha + ^{12}\text{C}$, $\alpha + ^{40}\text{Ca}$, both at $E_{\text{lab}} = 1370$ MeV.

B. Strong absorption model for elastic scattering

The first example is a simple SAM in which the S_l is directly parametrized by

$$S_l \equiv S(\lambda) = \frac{1}{1 + \exp(\frac{\Lambda - \lambda}{\Delta})} + \frac{1}{1 + \exp(\frac{\Lambda + \lambda}{\Delta})}, \quad (8)$$

with $\lambda = l + \frac{1}{2}$, $\Lambda = 10.0$ and $\Delta = 1.8$,

The SAM (with modifications for the Coulomb interaction, and in a slightly different form from (8)) was widely used in early studies of heavy-ion elastic scattering [21, 22]. At the present time, the SAM is not so popular, using either simple forms such as (8) or more sophisticated functions. It has been found that the characteristics of heavy-ion angular distributions, measured over wide angular ranges, are not accounted for by the simpler SAM models; instead the angular scattering is more easily described using optical potentials, rather than attempting complicated extensions of the SAM.

In spite of this, the SAM in its simple form (8) continues to be of interest, since it allows important tests of NF decompositions [12, 16, 17, 19]. This is because the PWS for the SAM (8) can be evaluated easily by saddle point techniques [12], or more simply, using the Watson transformation and elementary complex integration. Both methods allow a simple, mathematically correct, identification of the NF subamplitudes. For $\Lambda \gg 1$, $\exp(-2\pi\Delta) \ll 1$ and $\Lambda \sin \theta \gg 1$, it is found that the NF subamplitudes are $\propto \exp(-\pi\Delta\theta \mp i\Lambda\theta)/\sqrt{\sin \theta}$, to a good degree of approximation (Ref. [4], Eq. (3.5)). The NF cross sections, multiplied by $\sin \theta$ are equal and have an exponential slope, whereas the phase derivatives of the NF subamplitudes are expected to be equal to $\mp\Lambda$, respectively.

The results obtained by applying the Fuller NF method to the SAM with parameters $\Lambda = 10.0$ and $\Delta = 1.8$ are shown in Fig. 1. In the lower panel, we show a log plot of the dimensionless quantity $4k^2\sigma(\theta)\sin \theta$ versus θ since the corresponding NF quantities are expected to have an exponential slope. This is additionally shown in Fig.1 by the thin dot-dash line which represents $\log_{10}[\exp(-2\pi\Delta\theta)]$. Furthermore, because the S_l

are real, $f(\theta)$ has a constant phase (and its phase derivative is of no interest), while the $f^{(\mp)}(\theta)$ have identical moduli but opposite phases. Thus we need only show the N (or F) LAM and similarly for the cross sections. In Fig. 1, the N and F quantities are shown by thick continuous and dashed curves, respectively.

In a systematic notation explained in Sect. III, the results obtained from the Fuller NF method, which substitutes (3) into (1), are indicated by $R = 0$. The thin curve, in the lower panel of Fig. 1, shows the full cross section. Figure 1 shows that, for $R = 0$, unphysical contributions dominate the $F (= N)$ cross section over most of the angular range, i.e. for $\theta \gtrsim 50^\circ$. In particular, the F curve is completely different from the expected exponential decrease. Also the $F (= -N)$ LAM ≈ 0 for $\theta \gtrsim 50^\circ$. At forward angles, oscillations in the F LAM curve indicate that another F subamplitude is present, which interferes with the unphysical one. This behavior does not support the conjecture that the F LAM of this other subamplitude has the expected value, $\Lambda = 10.0$.

By comparing the lower panel of Fig. 1 with the corresponding Fig. 1 of [13], for which $\Lambda = 10$ and $\Delta = 2.0$, one observes that the change in Δ has not altered the magnitude of the unphysical contribution in the angular region where it is dominant. The explanation for this observation is straightforward. The amplitude obtained on dropping S_l from the term $S_l - 1$ in (2) is $f_\delta(\theta) = i\delta(1-x)/k$. Applying to $f_\delta(\theta)$ the same procedure used by Fuller to derive the NF Coulomb subamplitudes (Ref. [3], Eq. 11), we find that the NF components of $f_\delta(\theta)$ are $f_\delta^{(\mp)}(\theta) = \pm[2\pi k(1-x)]^{-1}$. The corresponding NF cross sections, downward shifted by one vertical unit, are shown in Fig. 1 by the thin dotted curve and labelled NF_δ . This curve shows that the major part of the unphysical contribution, when it dominates the Fuller F subamplitude, is due to $f_\delta^{(+)}(\theta)$ and does not depend on the properties of S_l .

A more satisfactory Fuller NF result is obtained by dropping 1 from the term $S_l - 1$ in (2), and then considering the PWS thus obtained as a distribution. To ensure convergence of the resulting NF subamplitudes, a YRW resummation is performed on them. This is explained in more detail in Sect. III, and in a systematic notation developed there, is denoted $R = 0_Y$. Figure 1 shows that the $R = 0_Y$ results are rather good at forward angles, $\theta \lesssim 70^\circ$. Apart from a small region around $\theta = 0^\circ$, where the condition $\Lambda \sin \theta \gg 1$ is not satisfied, the $N (= -F)$ LAM agrees closely with the expected value of $-\Lambda$ up to $\theta \approx 70^\circ$, and the $N (= F)$ cross section follows the expected exponential decrease. For $\theta \gtrsim 120^\circ$, the N cross section is still dominated by an unphysical contribution. At intermediate angles, $70^\circ \lesssim \theta \lesssim 120^\circ$, interference oscillations appear both in the N cross section and in the N LAM curve. It is interesting to note that the NF LAMs are more sensitive to interference effects in Fig. 1 than are the NF cross sections. Also, in the interference region, one cannot attach the meaning of a *local angular momentum* to the subamplitude phase

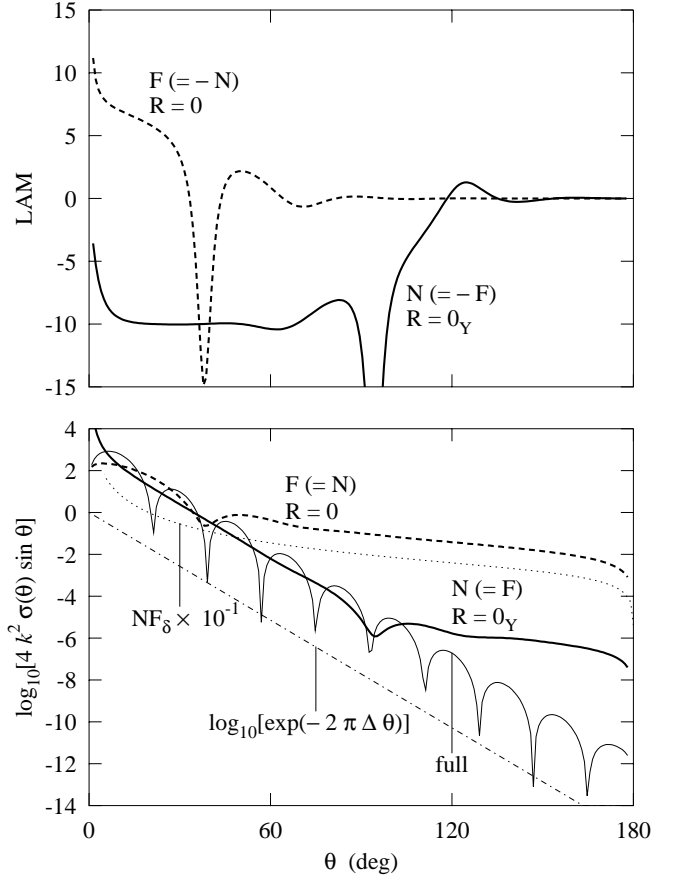


FIG. 1: Strong absorption model N (thick continuous curves) and F (thick dashed curves) cross sections (lower panel) and LAM (upper panel) calculated using the $R = 0$ and $R = 0_Y$ NF methods. The thin curve shows the full cross section. The thin dotted curve (NF_δ) shows the $F (= N)$ cross section for the unphysical amplitudes $f_\delta^{(\mp)}(\theta)$ (displaced downward by one unit). The thin dot-dashed line shows the slope of the expected exponential behavior for the NF cross sections

derivative. In our case, in this interference region, the N LAM curve oscillates around the expected semiclassical value of $-\Lambda$ in the region, $70^\circ \lesssim \theta \lesssim 90^\circ$, where the true semiclassical component dominates the N subamplitude, and around the unphysical value of 0 at larger angles.

C. Optical model for $^{16}\text{O} + ^{16}\text{O}$ elastic scattering

Figure 2 shows our results for the phenomenological (WS2) optical potential used to fit [7] the $^{16}\text{O} + ^{16}\text{O}$ elastic cross section at $E_{\text{lab}} = 145$ MeV. The usual Fuller NF method has been applied that employs an analytic formula for the NF subamplitudes of the Coulomb scattering amplitude [3]. The parameters for this potential are given in Table 1 of Ref. [7]. In the upper panel we display LAM/k , which we call the *Local Impact Parameter* (LIP), and in the lower panel a log plot of $\sigma(\theta) \sin \theta$. The thin continuous lines show the (unsymmetrized) cross

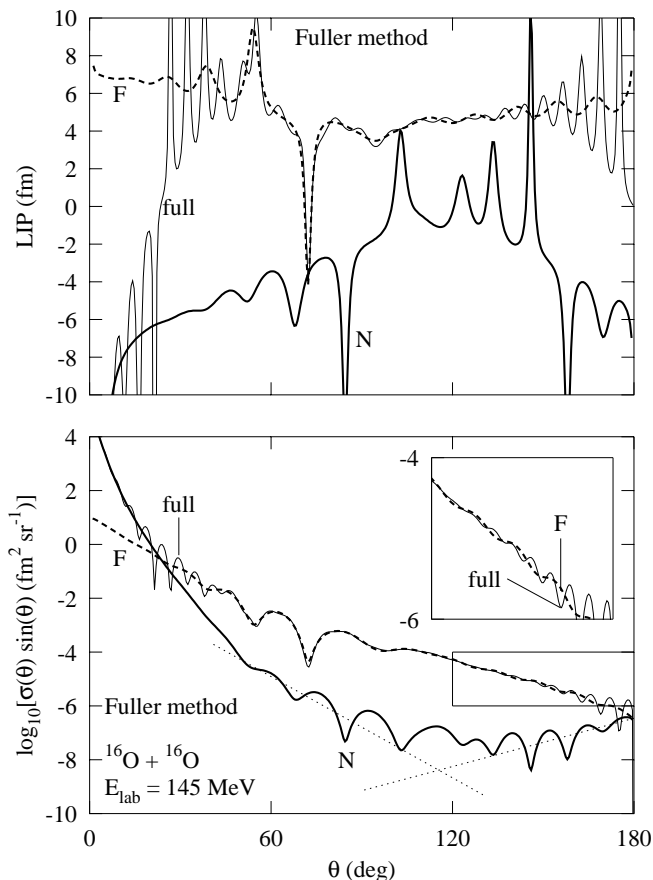


FIG. 2: Fuller N (thick continuous curves) and F (thick dashed curves) cross sections (lower panel) and LIP (upper panel) for $^{16}\text{O} + ^{16}\text{O}$ elastic scattering at $E_{\text{lab}} = 145$ MeV. The thin continuous curves show the cross section and LIP using the full amplitude. The two thin dotted lines show interpolations of the average behavior of the N cross section in the ranges $50^\circ \leq \theta \leq 90^\circ$ and $\theta \geq 150^\circ$. The inset in the lower panel shows a vertical magnification by a factor of 3 of the thin rectangular area.

section and LIP for the full amplitude. For $\theta \approx 20^\circ$, and at backward angles, the full cross section is characterized by oscillations having approximately the same period. In the intermediate angular range, $50^\circ \lesssim \theta \lesssim 150^\circ$, there are oscillations of longer period, which increases as θ increases. These properties, which are typical of light heavy-ion scattering, are much more complicated than those for the simple SAM cross sections, and indicate the presence of several interfering subamplitudes.

The oscillations in the LIP curve for the full amplitude qualitatively follow those in the full cross section. In addition, the change in sign of the full LIP for $\theta \approx 20^\circ$ indicates a crossover between one N subamplitude, dominant at smaller angles (where the full LIP oscillates around negative values), with a F subamplitude that is dominant at larger angles (where the full LIP oscillates around positive values). The oscillations of longer period in the intermediate angular range for the full cross section corre-

spond to an oscillating positive LIP. This indicates there is an interference between two F subamplitudes with a crossover near the deep minimum at $\theta \approx 70^\circ$. The oscillations at backward angles in the full cross section indicate an interference of one of these F subamplitudes with its continuation to the opposite side of the target (N).

The results of the Fuller NF method (thick curves, continuous for N and dashed for F quantities) in Fig. 2 confirm this interpretation. The N cross section crosses the F one at $\theta \approx 20^\circ$; the F cross section oscillates in the intermediate angular range before decreasing, almost monotonically, towards backward angles, where it meets the N cross section. For $\theta \gtrsim 60^\circ$, the behavior of the N cross section is characterized by rather complicated oscillations. It is difficult to imagine that these oscillations arise only from interference between a N subamplitude, which is dominant at forward angles, with a N subamplitude dominant at backward angles. The thin dotted lines in Fig. 2 show interpolations (linear fits) of the average behavior of the N cross section in the ranges $50^\circ \leq \theta \leq 90^\circ$ and $\theta \geq 150^\circ$. In the crossing region of the dotted lines, the N cross section is about two orders of magnitude larger than the crossing value. The contribution from an additional N subamplitude is apparently necessary to explain this behavior of the N cross section. The shape of the N LIP curve supports this conjecture. The N LIP curve is oscillatory, with increasing oscillation amplitude, up to $\theta \approx 85^\circ$, where the deep minimum corresponds to a crossover between two interfering N subamplitudes. For $85^\circ \lesssim \theta \lesssim 145^\circ$, the N LIP curve is oscillatory around 0, which suggests an unphysical origin for the N subamplitude dominant in this angular range. At $\theta \approx 145^\circ$, where there is a narrow maximum in the N LIP curve, the unphysical N subamplitude crosses a different N subamplitude, that becomes dominant at backward angles. Oscillations, similar to those observed at backward angles in the N LIP curve, are present at backward angles in the F LIP curve. The corresponding oscillations in the F cross section are barely visible with the scale used in the lower panel of Fig. 2. They can, however, be observed in the inset, where the thin rectangular area is plotted with a vertical scale magnified by a factor of 3.

In summary our detailed analysis of the NF LIP and NF cross sections indicates the presence of an unphysical contribution, which makes the properties of these quantities unnecessarily complicated.

D. Additional optical model examples

In this section we briefly discuss five additional examples where the NF optical potential cross sections are dominated by unphysical contributions over wide angular ranges.

Figure 3 shows N (upper panel) and F (middle panel) cross sections obtained by the usual Fuller NF method for different optical potentials that describe the elastic scattering of ^{16}O by ^{16}O , at $E_{\text{lab}} = 480, 704$ and 1120

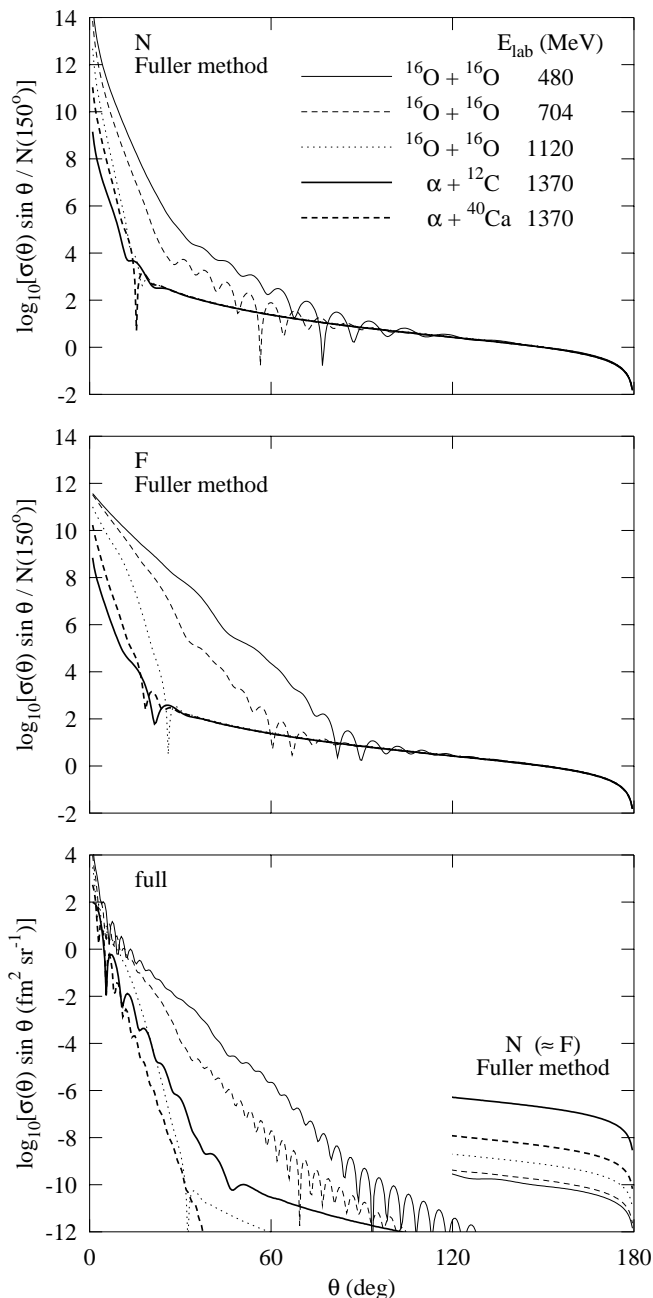


FIG. 3: Fuller N (upper panel) and F (middle panel) optical potential cross sections for $^{16}\text{O} + ^{16}\text{O}$, $\alpha + ^{12}\text{C}$ and $\alpha + ^{40}\text{Ca}$ at different energies. All the N and F curves are normalized to the values of the corresponding N quantities at $\theta = 150^\circ$. The lower panel shows the full cross sections and, for $\theta > 120^\circ$, the unphysical behavior of the Fuller N (\approx F) cross sections.

MeV (potentials labelled WS2 in Ref. [7]), and of α particles by ^{12}C and ^{40}Ca , at $E_{\text{lab}} = 1370$ MeV (potentials labelled WSa in Ref. [10]). We used relativistically corrected kinematics [23] in all these optical potential calculations, and symmetrisation effects were ignored for the $^{16}\text{O} + ^{16}\text{O}$ system.

In the N and F panels, we have normalized the quan-

ties, $\log_{10}[\sigma(\theta) \sin \theta]$, to the values of the corresponding N quantities, indicated by $N(\theta_0)$, at $\theta_0 = 150^\circ$. Except for a restricted region at forward angles, whose width depends on the system considered, the normalized Fuller NF cross sections are practically equal, for different colliding partners and/or energies. In every case, the unphysical effects of the Fuller NF method are as striking as those for the SAM discussed in Sect. II B. In the lower panel we have plotted, without normalization factors, the full cross sections and, for $\theta \geq 120^\circ$, the Fuller N (\approx F) cross section. It is very apparent that, at large angles, the behavior of the full cross sections is quite different from that of the Fuller NF cross sections. In particular, the $^{16}\text{O} + ^{16}\text{O}$ full cross sections at 480 MeV and 704 MeV possess a pronounced interference pattern in an angular region where the Fuller NF cross sections are dominated by unphysical contributions. For completeness, we remark that the NF LIP is practically null in the angular ranges where the NF cross sections show unphysical behavior for all these cases.

III. IMPROVED NF METHOD USING RESUMMATION

A. Resummation of full and NF PWS

In the preceding Section, we have discussed examples where the Fuller NF method resulted in unphysical contributions. We also clearly demonstrated that the Fuller method has the capability to identify the unphysical contributions through anomalous behavior in the NF LAM, or LIP. This capability helps us to avoid misleading interpretations of the full and NF cross sections obtained from the Fuller NF method. However the problem of finding more satisfactory NF methods without unphysical contributions remains open.

A possible solution to this problem was proposed by Hatchell [12], who used a modified NF method. The modifications consisted of, first, in writing $f(\theta)$ in the resummed form ($x \neq 1$)

$$f(\theta) = \frac{1}{2ik} \frac{1}{(1-x)^r} \sum_{l=0}^{\infty} a_l^{(r)} P_l(x), \quad (9)$$

$r = 1, 2, \dots$, and, second, in using a different splitting in the resummed PWS (9) for the Legendre polynomials into traveling waves.

The use of the resummed form (9) for $f(\theta)$ was originally proposed [14] by Yennie, Ravenhall, and Wilson (YRW) in a different context. Equation (9) is an exact resummation formula, of order r , which is derived from the recurrence relation for Legendre polynomials. Some mathematical properties of the resummed PWS (9) have been investigated by Wimp [24]. The YRW resummed form (9) can be derived by iterating r times, starting

from $a_l^{(0)} = a_l$, the resummation identity ($x \neq 1$)

$$\sum_{l=0}^{\infty} a_l^{(i-1)} P_l(x) = \frac{1}{1-x} \sum_{l=0}^{\infty} a_l^{(i)} P_l(x), \quad i = 1, 2, \dots, \quad (10)$$

where

$$a_l^{(i)} = -\frac{l}{2l-1} a_{l-1}^{(i-1)} + a_l^{(i-1)} - \frac{l+1}{2l+3} a_{l+1}^{(i-1)}, \quad (11)$$

with $a_{-1}^{(i-1)} = 0$.

It is important to remark that the resummed coefficients $a_l^{(r)}$, being linear combinations of the $a_l^{(0)} = a_l$, can have very different properties from the original physical a_l . However, no information about the physical a_l is lost on applying the resummation procedure, and the value of $f(\theta)$ does not depend in any way on the resummation order used. This is true for (9) and for all the resummed forms for $f(\theta)$ derived in this paper and is a consequence of the (exact) mathematical properties of the Legendre polynomials.

Equation (9) does not hold for a PWS written in terms of a linear combination of Legendre functions of integer degree of the first and second kinds ($x \neq \pm 1$)

$$\mathcal{F}(\theta) = \sum_{l=0}^{\infty} a_l \mathcal{L}_l(x), \quad (12)$$

where

$$\mathcal{L}_l(x) = p P_l(x) + q Q_l(x), \quad (13)$$

with p and q real or complex constants independent of l . Rather, as a result of the property $l Q_{l-1}(x) \rightarrow 1$ as $l \rightarrow 0$, the *extended* resummation identity holds ($x \neq \pm 1$) [25]

$$\sum_{l=0}^{\infty} a_l^{(i-1)} \mathcal{L}_l(x) = \frac{1}{1-x} \left[\sum_{l=0}^{\infty} a_l^{(i)} \mathcal{L}_l(x) - q a_0^{(i-1)} \right], \quad (14)$$

where the recurrence relation (11) gives $a_l^{(i)}$ in terms of $a_l^{(i-1)}$. By iterating (14) r times, $\mathcal{F}(\theta)$ can be written in the *extended* resummed form ($x \neq \pm 1$) [25]

$$\mathcal{F}(\theta) = \frac{1}{(1-x)^r} \sum_{l=0}^{\infty} a_l^{(r)} \mathcal{L}_l(x) - q \sum_{i=1}^r a_0^{(i-1)} \frac{1}{(1-x)^i}. \quad (15)$$

It is important to note that $\mathcal{F}(\theta)$ is independent of the value used for r .

The $Q_l^{(\mp)}(x)$ used to split $P_l(x)$ in the Fuller NF method are a particular case (with $p = 1/2$, and $q = \pm i/\pi$) of the more general linear combination $\mathcal{L}_l(x)$.

When the splitting (3) is made in the initial (1) or resummed PWS (9), different NF subamplitudes are obtained, i.e. the NF subamplitudes depend on the order

r of the resummation. In particular, the last term on the r.h.s. of (15) is omitted from these r dependent resummed NF subamplitudes. However, the sum of the NF resummed subamplitudes remains $f(\theta)$, because the differences exactly cancel each other. A different extended resummation identity occurs in the Hatchell approach, because the functions he used in place of the $Q_l(x)$ obey a (inhomogeneous) recurrence relation, different from that for $Q_l(x)$ (see Ref. [16] for details).

It is important to realize that the YRW resummation procedure (which has been extended in [25] to treat PWS like (12)) can also be used to speed up the convergence of the PWS (1) or (6), or even to ensure their convergence if the PWS was originally defined only in a distributional sense: in fact if $a_l \sim O(l^{-p})$ then $a_l^{(r)} \sim O(l^{-p-2r})$. Indeed the YRW resummation procedure was originally introduced [14] to produce, for $r \geq 1$, a convergent [26] PWS for the full amplitude of high-energy electron-nucleus scattering in which S_l is asymptotically Coulombic, and also to speed up the convergence of this PWS.

Using his splitting for $P_l(x)$ into traveling angular waves, Hatchell has shown [12] that the unphysical contributions to the SAM NF cross sections systematically decrease on increasing r , i.e. on using the resummed PWS (9) before the splitting of $P_l(x)$, rather than the original unresummed PWS (1). More recently [16, 17], it was shown that the same NF resummed method gives even better results if the Fuller $Q_l^{(\mp)}(x)$ functions are used. The superiority of the $Q_l^{(\mp)}(x)$ seems to be connected with the greater rapidity with which the $Q_l^{(\mp)}(x)$ approach their asymptotic behavior (7) [15, 16, 17], compared to the Hatchell NF functions.

The success of using (9) before applying the NF splitting (3) depends upon the properties of the resummed coefficients $a_l^{(r)}$. For the SAM at low l values, the $a_l^{(r)}$ rapidly decrease in magnitude [16] with increasing r . As a result, the low l values, where the splitting into running angular waves is physically less reasonable, give a smaller contribution to the resummed PWS.

However, in some cases, this resummation technique acts in the opposite direction, by enhancing the undesired unphysical contributions to the NF resummed subamplitudes. We have found that this happens, for example, for pure Coulomb scattering, for scattering by an impenetrable sphere, and for the SAM (see [19]) when the cross section is calculated at an angle $\pi - \theta$, using the identity $P_l[\cos(\pi - \theta)] = (-1)^l P_l(\cos \theta)$.

B. Improved resummation of full and NF PWS

One possible solution to the intriguing puzzle discussed in Section III A is to regard (10) as a particular case of

the modified resummation identity [18]

$$\sum_{l=0}^{\infty} a_l^{(i-1)} P_l(x) = \frac{1}{\alpha_i + \beta_i x} \sum_{l=0}^{\infty} a_l^{(i)} P_l(x), \quad i = 1, 2, \dots, \quad (16)$$

with $\alpha_i + \beta_i x \neq 0$ and

$$a_l^{(i)} = \beta_i \frac{l}{2l-1} a_{l-1}^{(i-1)} + \alpha_i a_l^{(i-1)} + \beta_i \frac{l+1}{2l+3} a_{l+1}^{(i-1)}. \quad (17)$$

For $\alpha_i, \beta_i \neq 0$, apart a renormalization factor, the r.h.s. of (16) depends only on the ratio β_i/α_i . Thus, without loss of generality, we can assume $\alpha_i = 1$ for all i . By iterating (16) r times, we can write $f(\theta)$ in the modified resummed form ($1 + \beta_i \neq 0$)

$$f(\theta) = \frac{1}{2ik} \left(\prod_{i=1}^r \frac{1}{1 + \beta_i x} \right) \sum_{l=0}^{\infty} a_l^{(r)} P_l(x), \quad (18)$$

$r = 1, 2, \dots$. It is straightforward to show that the extended modified resummed form for the PWS (12) is given by ($x \neq \pm 1$ and $1 + \beta_i \neq 0$)

$$\begin{aligned} \mathcal{F}(\theta) = & \left(\prod_{i=1}^r \frac{1}{1 + \beta_i x} \right) \sum_{l=0}^{\infty} a_l^{(r)} \mathcal{L}_l(x) \\ & + q \sum_{i=1}^r \beta_i a_0^{(i-1)} \prod_{j=1}^i \frac{1}{1 + \beta_j x}. \end{aligned} \quad (19)$$

The identity (18) is the key result for our improved NF method. The YRW resummation formula (9) is obtained when $\beta_1 = \beta_2 = \dots = \beta_r = -1$.

The resummed form (18) with $\beta \equiv \beta_1 = \dots = \beta_r$ is a particular case of a more general one [18], which uses a basis set of reduced rotation matrix elements; this gives the amplitude for more general scattering processes than those described by (1). For these general PWS, a Fuller-like NF decomposition can be introduced [27, 28, 29] which allows the scattering amplitude to be separated into NF subamplitudes. In some cases, the NF cross sections contained unexpected (unphysical) oscillations [18], which are enhanced if the generalization of (9) is used, but which disappear for an appropriate choice of the β -parameter in the generalization of (18).

The considerable successes achieved by the original Fuller NF method suggest that the modified resummed form (18) be used to diminish unphysical contaminations to the NF subamplitudes when they are present. To do this, we must give a practical rule to fix the values of the β_i parameters. In Refs. [18, 19], it was proposed to select the value of $\beta \equiv \beta_1 = \dots = \beta_r$ so that $(1 + \beta x)^{-r}$ *approximately mimics the shape of the angular distribution*. The shape of the cross section can however be very different from that given by $(1 + \beta x)^{-r}$. It is therefore desirable to test a different recipe, based on a simple rule. The quantitative recipe proposed here is inspired by the observation that the modified resummation procedures

produce a more physical NF understanding by reducing the contribution from the low l values in the resummed PWS. This suggests that we select the $\beta_1, \beta_2, \dots, \beta_r$ in r repeated applications of (16), so as to eliminate as many low l terms as possible from the resummed PWS in (18).

The transformation from $\{a_l^{(i-1)}\}$ to $\{a_l^{(i)}\}$ is linear tridiagonal, with coefficients linear in β_i , which means that a resummation of order r allows one to equate to zero the leading r coefficients $a_l^{(r)}$, with $l = 0, 1, \dots, r-1$, by solving a system of r equations of degree r in the parameters $\beta_1, \beta_2, \dots, \beta_r$. We will call the resummation defined in this way an *improved resummation of order r* .

It is straightforward to show that the improved resummation of order $r = 1$ is obtained by choosing

$$\beta_1 = -3a_0/a_1, \quad (20)$$

while the improved resummation of order $r = 2$ is given by

$$\beta_{1,2} = (B \pm \sqrt{B^2 - 4A})/2, \quad (21)$$

with A and B solutions of the linear equations

$$\begin{cases} (\frac{1}{3}a_0 + \frac{2}{15}a_2)A + \frac{1}{3}a_1B = -a_0 \\ (\frac{3}{5}a_1 + \frac{6}{35}a_3)A + (a_0 + \frac{2}{5}a_2)B = -a_1. \end{cases} \quad (22)$$

Higher order improved resummations require the solution of more complicated systems of equations.

Note that the improved resummation of order $r = 1$ is, obviously, not defined if $a_1 = 0$. Similarly the resummation of order $r = 2$ is not defined for an (accidentally) zero value of the determinant of the linear equations (22). Analogous limitations are expected to hold for higher order resummations. However, these pathological situations were never observed in our calculations. In all the cases we have analyzed using $r \leq 2$, we find that the improved resummations considerably reduce the width of the angular regions in which the Fuller NF cross sections exhibit unphysical behavior. In these analyses, we have used S_l from simple parametrizations, as well as from some of the optical potentials currently employed to describe light heavy-ion scattering.

Note that, as for the YRW resummed form (9), no physical information is lost on using our improved resummed form (18), and the full $f(\theta)$ does not depend in any way on the resummation order used. This might seem surprising, because our method omits the contribution from low values of l . For example, for the improved resummation of order $r = 1$, the *resummed* term $a_0^{(1)}$ is set to zero in the *resummed* PWS, but the information on the *physical* value of a_0 is contained in the *resummed* term $a_1^{(1)}$ and in the resummation parameter β_1 , and similarly for higher order resummations. The improved resummation method only modifies the NF (resummed) subamplitudes, not their sum $f(\theta)$, as it tries to eliminate unphysical contributions that have their origin in the NF splitting of the $P_l(x)$ into running waves $Q_l^{(\mp)}(x)$.

The physical meaning of the NF splitting (3) is based on the asymptotic properties of $P_l(x)$ and $Q_l^{(\mp)}(x)$, see (7). The NF splitting (3) is not expected to be physically meaningful for low l values. For example, for $l = 0$, (3) states that $P_0(x) = 1$ is the sum of

$$Q_0^{(\mp)}(x) = \frac{1}{2} \pm \frac{i}{2\pi} \ln[(1+x)/(1-x)]. \quad (23)$$

This decomposition of unity is undoubtedly mathematically exact, but it is difficult to think that it can be physically meaningful. It is contributions of this type that the improved resummation omits from the resummed PWS, after having moved to higher values of l in the resummed PWS, the physical information contained in the original S_l .

It is also interesting to understand the reasons for the successes and failures of the Hatchell method for the SAM [16, 17, 19] based on the use of the YRW resummed form (9) for $f(\theta)$ and the Fuller NF splitting (3). In those cases where the Hatchell method is successful, we find for low l values, $S_l \approx S_{l+1}$, and the $a_l^{(r)}$ are made small in magnitude with the choice $\beta_1 \approx \beta_2 \approx \dots \approx \beta_r \approx -1$. In those cases where the Hatchell method fails, it happens that, for low l values, $S_l \approx -S_{l+1}$, and the choice $\beta_1 \approx \beta_2 \approx \dots \approx \beta_r \approx 1$ makes the $a_l^{(r)}$ small in magnitude. Our improved method automatically chooses appropriate values for the resummation parameters using the exact values of S_l .

Finally, we summarize the procedure used by our new improved resummation method. The calculations are performed applying: *first*, an improved resummation of order $r = 0, 1, 2$, with $r = 0$ meaning no resummation, *second*, the Fuller NF splitting (3), and *third* an extended YRW resummation (15) of the NF (resummed) subamplitudes. This latter YRW resummation is necessary to ensure the convergence of the final NF PWS. This final resummation can, however, be replaced with any other procedure that provides convergence of the final NF PWS. The results obtained from these three steps will be indicated by the notation $R = 0_Y, 1_Y, 2_Y$. The notation $R = 0_Y$ is used in Fig. 1. Also, we use $R = 0$ to indicate the original Fuller method for the SAM case: no resummation and no final YRW resummation, because, in this case, the presence of the 1 in the term $S_l - 1$ ensures rapid convergence of the PWS.

C. Strong absorption model for elastic scattering

Our results obtained after applying the $R = 1_Y, 2_Y$ procedures to the SAM of Sec. II B are shown in Fig. 4. The effectiveness of the improved resummation procedure is impressive, both for the NF cross sections and for the NF LAM curves. Using the $R = 1_Y$ method (for which $\beta_1 = -0.7621$), the $F (= -N)$ LAM and the $F (= N)$ cross section are in agreement with the expected results up to $\theta \approx 140^\circ$. For $R = 2_Y$ (which has

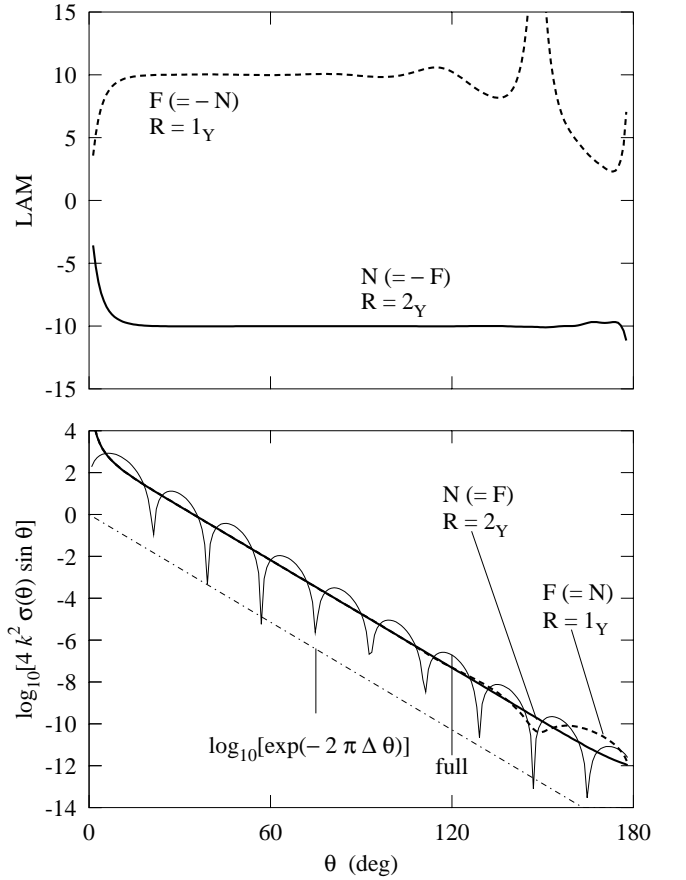


FIG. 4: Same as Fig. 1, except using the $R = 1_Y, 2_Y$ resummation methods.

$\beta_{1,2} = -0.8634 \pm 0.0723 i$), the agreement covers almost the whole angular range. The small irregular oscillations appearing at large θ for the N LAM curve, when $R = 2_Y$, may arise from precision limitations (64 bit floating point representation) in the calculations, or from residual unphysical contributions not completely removed by our improved method.

If instead we apply the YRW resummation procedure, we find that it gives worse results compared to our $R = 1_Y, 2_Y$ methods, although better results than the Fuller $R = 0_Y$ method. This is because the YRW choice of $\beta_1 = \beta_2 = -1$ is not too far from our improved estimate of these parameters.

Note that, using our improved procedure, the value of the SAM cut-off parameter, $\Lambda = 10$, is correctly identified in the plots of the LAM. Also, no shift of the LAM occurs on changing the resummation order. We recall that resummation does not change or translate in any way the physical properties S_l ; nor does it alter the physical content of $f(\theta)$. It only changes the coefficients $\alpha_l^{(r)}$ in the resummed PWS (18). Note that the $\alpha_l^{(r)}$ have a different meaning from the partial wave amplitudes a_l , and the summation index of the resummed PWS (18) should not be identified as the orbital angular momentum quantum

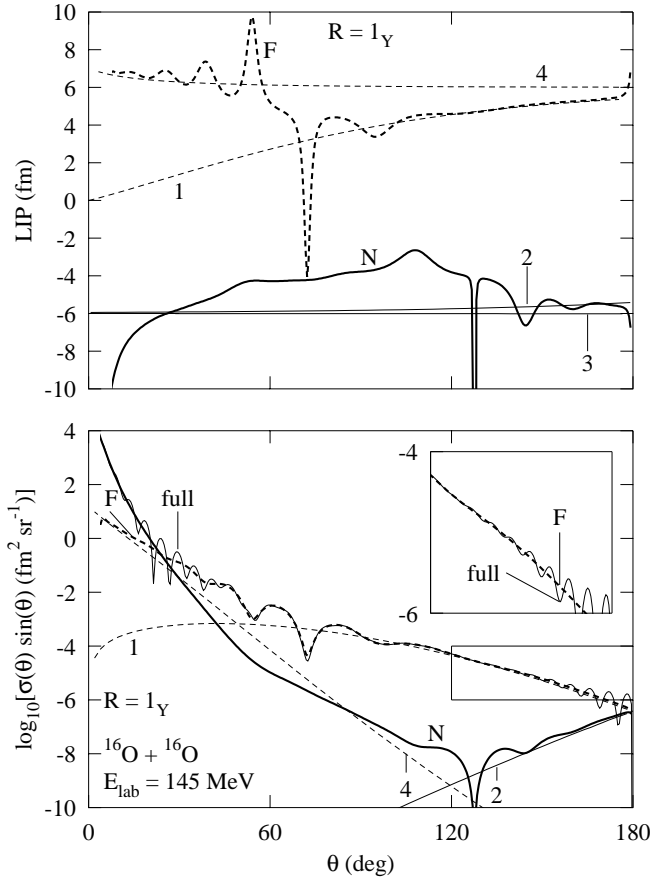


FIG. 5: Same as Fig. 2 except using the $R = 1_Y$ NF resummation method and the full LIP curve is not shown. Cross sections and LIP calculated using classical mechanics are shown by thin curves (continuous for N and dashed for F contributions). The indices 1, 2, 3 and 4 identify the curves corresponding to different branches of the classical deflection function.

number. This is because the resummation extracts the factor $\prod_{i=1}^r (1 + \beta_i x)^{-1}$ from the Legendre polynomial PWS.

D. Optical model for $^{16}\text{O} + ^{16}\text{O}$ elastic scattering

Figure 5 shows our results for the WS2 optical potential of Sec. II C using the $R = 1_Y$ method (for which $\beta_1 = -0.9997 - 0.0800i$). The oscillations of the Fuller N curves around $\theta \simeq 90^\circ$ are removed, and both the $R = 1_Y$ N cross section and the N LIP curve are considerably simpler than those from the Fuller method. The F curves are essentially the same as those in Fig. 2, although the $R = 1_Y$ method has suppressed the oscillations in the F cross section at backward angles (compare the insets in the lower panels of Figs. 2 and 5), as well as the oscillations in the F LIP curve in the same angular range. This demonstrates that the $R = 1_Y$ method is more effective than the usual Fuller one in decomposing $f(\theta)$ into slowly

varying NF subamplitudes. It also shows that some oscillations in the Fuller NF cross sections in Fig. 2 are artifacts, without any physical meaning, introduced by the properties of the NF technique used. We have also applied the improved resummation method $R = 2_Y$. The results are practically the same as those for $R = 1_Y$ and are not shown.

The cleaning by the $R = 1_Y$ procedure in Fig. 5 of the original Fuller NF subamplitudes (Fig. 2) is impressive and allows a better identification, in the F cross section and F LIP of the dominance, for $\theta \gtrsim 90^\circ$, of the contributions from classical-like trajectories refracted from the internal part of the nuclear interaction. In Fig. 5, this interpretation is demonstrated by the overall agreement, for $\theta \gtrsim 90^\circ$, between the F curves and the classical mechanical results (thin curve, labelled 1) corresponding to impact parameters smaller than the classical orbiting one.

For the WS2 potential the collision energy is, in fact, slightly below the critical energy at which orbiting disappears for the classical deflection function (when it is transformed into a nuclear rainbow minimum). Because of this, the dependence of the impact parameter b on θ is that of an infinitely many-valued function ([30], p. 127-129). Four of these branches, corresponding to the deflection function being larger than -360° , are plotted for the LIP in the upper panel of Fig. 5 (shown by thin curves) and labelled from 1 to 4 for increasing values of b . The LIP is assumed to be equal to b for the F branches (thin dashed curves, with labels 1 and 4) and to $-b$ in the N case (thin continuous curves, 2 and 3). In the lower panel, the thin curves, with the same labels, show the contributions to the classical cross section from these branches, in which we have included, in the usual simple way ([1], p. 49), the absorptive effects of the imaginary part of the optical potential.

The agreement between the quantum $R = 1_Y$ F curves and the classical curve labelled 1 is overall good for $\theta \gtrsim 90^\circ$, and is impressive for $\theta \gtrsim 120^\circ$. This shows that the $R = 1_Y$ F subamplitude, calculated by an exact quantum method, is dominated for $\theta \gtrsim 90^\circ$ by a classical contribution corresponding to trajectories with small impact parameters, $b \lesssim 5$ fm, which are refracted by the nuclear interaction. The contribution from F branch 1 continues at 180° into the contribution from N branch 2. However, as θ decreases from 180° , there is an increasing disagreement with the average quantum N contribution. Evidently, for impact parameters that approach the orbiting one ($b_{\text{orb}} = 6.001$ fm), diffractive effects start to become significant. Finally, we note that there is a large disagreement between the classical F curve 4 and the average behavior of the quantum F cross section at forward angles. This suggests that the other F subamplitude responsible for the interference pattern in the F quantum cross section cannot be considered a classical-like refractive contribution.

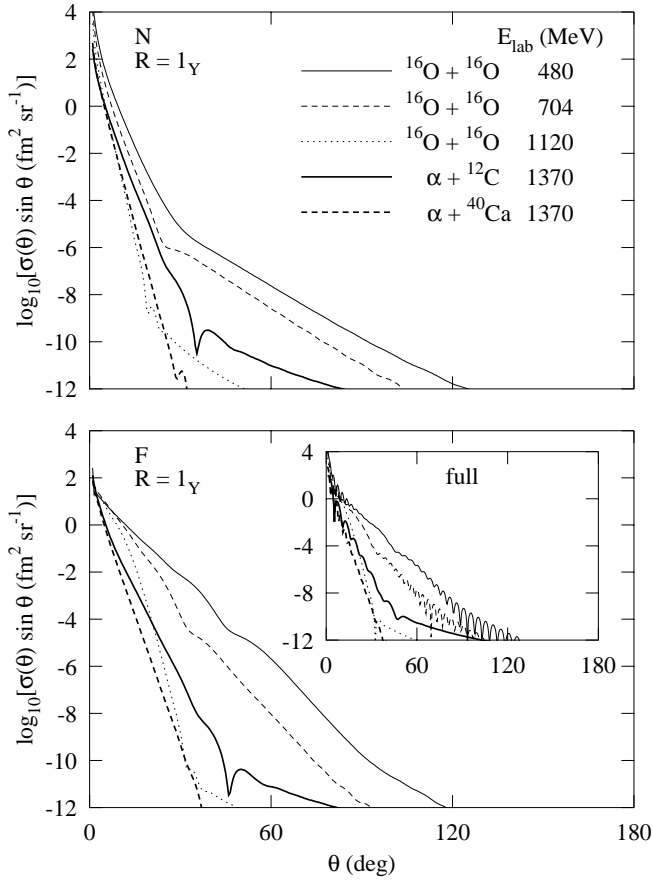


FIG. 6: Same as for the upper and middle panels of Fig. 3, except without normalization factors and the $R = 1_Y$ NF resummation method has been used. The inset shows the full cross sections.

E. Additional optical model examples

In Fig. 6, we show the N (upper panel) and F (lower panel) cross sections calculated using the improved NF method, $R = 1_Y$, for the optical potentials considered in Sec. IID. In contrast to Fig. 3, no normalization factors are used in Fig. 6. Comparison of Fig. 6 with Fig. 3 shows that the $R = 1_Y$ NF resummation method has removed the unphysical contributions that dominate the Fuller NF cross sections over most of the angular range.

For these cases, $\beta_1 = -1.0001 - 0.0283i, -1.0001 - 0.0218i, -0.9991 - 0.0102i, -0.9958 - 0.0021i$, and $-0.9985 - 0.0010i$, in descending order for the collision systems listed in the legend of the upper panel of Fig. 6. In all cases, $\beta_1 \approx -1$, which is a consequence of the fact that, for these five collision systems, at low l values we have $S_l \approx S_{l+1}$. The result $\beta_1 \approx -1$ also explains why the unphysical contributions in the Fuller NF cross sections of Fig. 3 have very similar shapes. Indeed for $\beta_1 = -1$, the angular dependence of the unphysical cross sections is $\propto (1-x)^{-2} \propto \sin^{-4}(\theta/2)$, which is the same as the Rutherford cross section. This implies that on making the (usual) plot of the ratio of the cross sections

to the Rutherford one, the unphysical contributions will appear independent of θ , i.e. a constant.

Figure 6 clearly shows that the $R = 1_Y$ method has cleaned the Fuller NF cross sections of unphysical contributions. The $R = 1_Y$ and Fuller NF cross sections agree closely at forward angles, with the $R = 1_Y$ curves providing the correct continuation of the Fuller NF curves to larger angles, where the unphysical Fuller NF contributions become dominant over the $R = 1_Y$ results. In addition, the $R = 1_Y$ procedure clearly identifies the oscillatory pattern of the $^{16}\text{O} + ^{16}\text{O}$ full cross sections at $E_{\text{lab}} = 480$ MeV and 704 MeV as an interference between the NF resummed subamplitudes.

As a final curiosity, we note that a 'suspect' behavior appears in the $R = 1_Y$ NF cross sections for $\alpha + ^{12}\text{C}$ at $\theta \gtrsim 40^\circ$. We find that the corresponding $R = 1_Y$ NF LIP are ≈ 0 for $\theta \gtrsim 60^\circ$. However, the LIP for the full amplitude is also ≈ 0 for $\theta \gtrsim 60^\circ$, indicating that the full cross section is dominated by contributions from low partial waves in this angular region.

We have repeated the calculations, substituting the WS form factors used in [10], with symmetrized WS-like form factors defined by

$$f_{\text{sym}}(r, R, d) = \sinh \frac{R}{d} / (\cosh \frac{R}{d} + \cosh \frac{r}{d}), \quad (24)$$

where R and d are the radius and diffuseness parameters, respectively. We find that the full cross section decreases for $\theta \gtrsim 60^\circ$ by more than 5 orders of magnitude, which exceeds the precision limits of our optical potential computer code. At forward angles the effect of the substitution is very small. This supports the conjecture that the suspect behavior in the $R = 1_Y$ NF and full cross sections arises from the 'cusp', which the usual WS potentials have at the origin. The cusp is expected to produce diffraction scattering for the low partial waves, which is equally distributed between the N and F subamplitudes. It is this effect that we observe, and which disappears on removing the cusp. Similar effects, although masked by the limited range of the scale along the ordinate, are also observed in the $^{16}\text{O} + ^{16}\text{O}$ collision at $E_{\text{lab}} = 1120$ MeV, as well as tentatively in the $R = 1_Y$ N $\alpha + ^{40}\text{Ca}$ cross section.

IV. CONCLUSIONS

Our new NF resummation procedure clearly improves the original Fuller NF method, as is evident from the seven examples discussed here, and from those presented elsewhere [13, 31]. In all these cases, we obtain NF resummed cross sections that are more slowly varying and less structured than the Fuller ones. On the one hand, our results confirm the utility of NF methods for gaining insight into the properties of the subamplitudes responsible for complicated structures in cross sections. On the other hand, they remind us of the empirical origin of NF

methods, and suggest caution in the interpretation of results obtained from NF techniques. Using different NF methods lets us check what parts of the resulting NF sub-amplitudes are independent of the particular technique used. Only properties stable with respect to different NF methods, can be considered as manifestations of some physical phenomenon.

In addition, we have shown that in all NF analyses, it is desirable to investigate the behavior of the LAM. This quantity is more sensitive to interference effects than are the NF cross sections, and a null value (or an oscillatory behavior around zero) of the NF LAM in a certain angu-

lar range may indicate the dominance of an unphysical contribution.

Acknowledgments

Support of this research by a PRIN MIUR (I) research grant, the Engineering and Physical Sciences Research Council (UK) and INTAS (EU) is gratefully acknowledged.

-
- [1] D. M. Brink, *Semi-Classical Methods for Nucleus-Nucleus Scattering* (Cambridge University Press, Cambridge, England, 1985).
 - [2] H. M. Nussenzweig, *Diffraction Effects in Semiclassical Scattering* (Cambridge University Press, Cambridge, England, 1992).
 - [3] R. C. Fuller, Phys. Rev. C **12**, 1561 (1975).
 - [4] M. S. Hussein and K. W. McVoy, Progr. Part. Nucl. Phys. **12**, 103 (1984).
 - [5] M. E. Brandan and G. R. Satchler, Phys. Rep. **285**, 143 (1997).
 - [6] M. P. Nicoli, F. Haas, R. M. Freeman, N. Aissaoui, C. Beck, A. Elanique, R. Nouicer, A. Morsad, S. Szilner, Z. Basrak, M. E. Brandan and G. R. Satchler, Phys. Rev. C **60**, 064608 (1999).
 - [7] D. T. Khoa, W. von Oertzen, H. G. Bohlen, and F. Nuoffer, Nucl. Phys. A **672**, 387 (2000).
 - [8] A. A. Ogloblin, Yu. A. Glukhov, W. H. Trzaska, A. S. Dem'yanova, S. A. Goncharov, R. Julin, S. V. Klebnikov, M. Mutterer, M. V. Rozhkov, V. P. Rudakov, G. P. Tiorin, Dao T. Khoa and G. R. Satchler, Phys. Rev. C **62**, 044601 (2000).
 - [9] S. Szilner, M. P. Nicoli, Z. Basrak, R. M. Freeman, F. Haas, A. Morsad, M. E. Brandan, and G. R. Satchler, Phys. Rev. C **64**, 064614.
 - [10] D. T. Khoa, G. R. Satchler, and N. D. Thuy, Phys. Rev. C **65**, 024611 (2002).
 - [11] A. A. Ogloblin, D. T. Khoa, Y. Kondo, Y. A. Glukhov, A. S. Dem'yanova, M. V. Rozhkov, G. R. Satchler, and S. A. Goncharov, Phys. Rev. C **57**, 1797 (1998).
 - [12] P. J. Hatchell, Phys. Rev. C **40**, 27 (1989).
 - [13] R. Anni, J. N. L. Connor, and C. Noli (2001), nucl-th/0111060.
 - [14] D. R. Yennie, D. G. Ravenhall, and R. N. Wilson, Phys. Rev. **95**, 500 (1954).
 - [15] P. McCabe and J. N. L. Connor, J. Chem. Phys. **104**, 2297 (1995).
 - [16] J. J. Hollifield and J. N. L. Connor, Molec. Phys. **97**, 293 (1999).
 - [17] J. J. Hollifield and J. N. L. Connor, Phys. Rev. A **59**, 1694 (1999).
 - [18] T. W. J. Whiteley, C. Noli, and J. N. L. Connor, J. Phys. Chem. A **105**, 2792 (2001).
 - [19] C. Noli and J. N. L. Connor, Zh. Fiz. Khim. (2002), (in press).
 - [20] J. R. Taylor, Nuovo Cimento B **23**, 313 (1974).
 - [21] W. E. Frahn, *Treatise on Heavy-Ion Science*, vol. 1, Elastic and Quasi-Elastic Phenomena, edited by D. A. Bromley (Plenum Press, New York, 1984), chap. 2.
 - [22] M. E. Grypeos, C. G. Koutroulos, V. K. Lukyanov, and A. V. Shebeko, Fiz. Element. Chast. Atom. Yadra **32**, 1494 (2001) [English translation: Phys. Part. Nucl. **32**, 779 (2001)].
 - [23] M. E. Farid and G. R. Satchler, Phys. Lett. B **146**, 389 (1984).
 - [24] J. Wimp, Num. Algorithms **21**, 377 (1999).
 - [25] R. Anni and L. Renna, Lett. Nuovo Cimento **30**, 229 (1981).
 - [26] D. M. Goodmanson and J. R. Taylor, J. Math. Phys. **21**, 2202 (1980).
 - [27] A. J. Dobbyn, P. McCabe, J. N. L. Connor, and J. F. Castillo, Phys. Chem. Chem. Phys. **1**, 1115 (1999).
 - [28] D. Sokolovski and J. N. L. Connor, Chem. Phys. Lett. **305**, 238 (1999).
 - [29] P. McCabe, J. N. L. Connor, and D. Sokolovski, J. Chem. Phys. **114**, 5194 (2001).
 - [30] R. G. Newton, *Scattering Theory of Waves and Particles*, 2nd edition, (Springer, New York, 1982).
 - [31] R. Anni, Eur. Phys. J. A (2002), (in press).